Polarized-neutron study of $TmCo_2$†

D. Gignoux, D. Givord, and F. Givord
Laboratoire de Magnétisme, Centre National de la Recherche Scientifique, Boîte Postale 166-X, 38042-Grenoble-Cedex, France

W. C. Koehler and R. M. Moon
Solid State Division, Oak Ridge National Laboratory, Oak Ridge, Tennessee 37830

(Received 5 January 1976)

Diffraction experiments with polarized neutrons have been carried out on a $TmCo_2$ single crystal, at various temperatures, in a field of 57.2 kOe applied parallel to the $[01\bar{1}]$ direction. The localized moments on Tm and Co sites have been determined at 4.2 and 100 K from the magnetic densities obtained by Fourier projections. The Tm moment ($5.4\mu_B$ at 4.2 K) is reduced by crystal-field effects. A $3d$-type Co moment is coupled antiparallel to the Tm one. The magnetic scattering amplitudes measured for the reflections to which the $4f$ Tm moment does not contribute give direct evidence for the existence of a diffuse magnetic density. This diffuse density is oscillatory with distance and remains similar at all temperatures. The $4f$ Tm and the $3d$ Co moments have been evaluated at eight temperatures from 4.2 to 250 K. The Co susceptibility above 25 K is temperature independent. The Co behaves as a Pauli paramagnet under the action of two opposite fields: the molecular field due to Tm atoms and the applied field. A collective-electron model is therefore appropriate for the description of paramagnetic susceptibility. At 4.2 K a large increase of the Co susceptibility in the molecular field leads to a value of the Co moment of $0.8\mu_B$. This result can be related to the increase of the susceptibility observed in YCo_2 in high applied fields and to the first-order ferri-paramagnetic transition of some RCo_2 compounds, where R stands for rare-earth metals.

I. INTRODUCTION

The intermetallic compounds of rare-earth metals (R) and transition metals (M = Fe, Co, Ni) are divided into two groups with quite different magnetic properties.[1] In the rare-earth-rich alloys (RNi, R_4Co_3, R_3Ni, R_3Co) the transition metal is not magnetic; ordering temperatures are below room temperature and are determined by oscillatory interactions of the Rudermann-Kittel type between rare-earth atoms. In the transition-metal-rich alloys (R_2M_{17}, RCo_5, R_2Co_7, RFe_3, RCo_3, and RFe_2), the transition-metal atoms carry an intrinsic magnetic moment which is always antiparallel to the spin of the rare-earth atom. Compounds are then ferromagnetic with the light rare earths and ferrimagnetic with the heavy ones. Resulting interactions are strong, leading to high ordering temperatures, often above room temperature. In the RCo_2 compounds, whose properties are intermediate to those of these two groups, the appearance of $3d$ magnetism is observed. YCo_2 and $LuCo_2$ exhibit a strong Pauli paramagnetism,[2,3] while with magnetic rare earths, a magnetic moment on cobalt atoms is created by the magnetic interactions due to the rare-earth atoms[4] [$1\mu_B$/(Co atom) in $GdCo_2$]. The magnetic ordering transitions of $DyCo_2$, $HoCo_2$, and $ErCo_2$ are of first order[2,5,6] and they have been interpreted by a model of itinerant electron metamagnetism, produced by the rare-earth–cobalt interactions.[7]

The thermal variation of the RCo_2 paramagnetic susceptibility has been interpreted with two different models.[8,9] In the first representation, R and Co atoms carry intrinsic magnetic moments[8] which are disordered by the thermal effect. This is the classical model of ferrimagnetism, and the paramagnetic susceptibility follows a Néel-type law. In the collective-electron theory (Stoner model) the Co moment is induced by the field and the interactions with neighboring magnetic atoms. The paramagnetic susceptibility is enhanced[9] as in YCo_2.

Magnetic properties of $TmCo_2$ have been studied on a spherical single crystal.[10] The ordering temperature is 7 K. Below this temperature the easy magnetization axis is [111] and the hardest one is [100]. The Tm^{3+} ground state, deduced from these measurements, is the Γ_1 singlet. A previous neutron diffraction study on a polycrystalline sample[11] has confirmed the ferrimagnetic character of $TmCo_2$ and has given magnetic moments of $(3.20 \pm 0.13)\mu_B$/(Tm atom) and $(0.48 \pm 0.11)\mu_B$/(Co atom) at 1.5 K.

The polarized-neutron study of $TmCo_2$ should enable us to separate the different contributions to the magnetic density: the $4f$ localized Tm moment, the $3d$ Co moment, and a possible diffuse density. A study of the temperature and field dependence of the Co sublattice magnetization in the paramagnetic region should bring us information on the nature of the Co magnetism, that is, whether it is intrinsic local or collective electron magnetism.

II. EXPERIMENTAL

$TmCo_2$ crystallizes in the cubic $MgCu_2$-type Laves phase structure. A single-crystal button was prepared by the Bridgman method. The sample was spark cut into a parallelepiped $6 \times 1.2 \times 1.2$ mm^3, with its long dimension along the [01$\bar{1}$] axis. Magnetization along this direction and along the easy magnetization [111] direction was measured at the Service National des Champs Intenses (Grenoble) in fields up to 120 kOe at 4.2 K (Fig. 1), and in the paramagnetic region.

In order to refine the crystallographic structure, a preliminary study at room temperature was performed with unpolarized neutrons on the four-circle spectrometer HB-2 of the Oak Ridge High Flux Isotope Reactor (HFIR). The intensities of all Bragg reflections out to $(\sin\theta)/\lambda = 0.7$ Å^{-1} were measured.

All the polarized-beam measurements were made at the HB-1 triple-axis spectrometer of the HFIR. The sample was mounted in a cryostat designed so that the specimen could be rotated about its vertical [01$\bar{1}$] axis by means of external controls. Experiments were performed between 4.2 and 250 K; the temperature was defined to within 0.1 K. A magnetic field up to 57.2 kOe, created by a superconducting split coil, was applied normal to the scattering plane and parallel to the [01$\bar{1}$] axis of the specimen. As discussed further, the magnetization in 57.2 kOe is collinear to the applied field at all temperatures.

The polarized-beam technique yields, in principle, the polarization ratio:

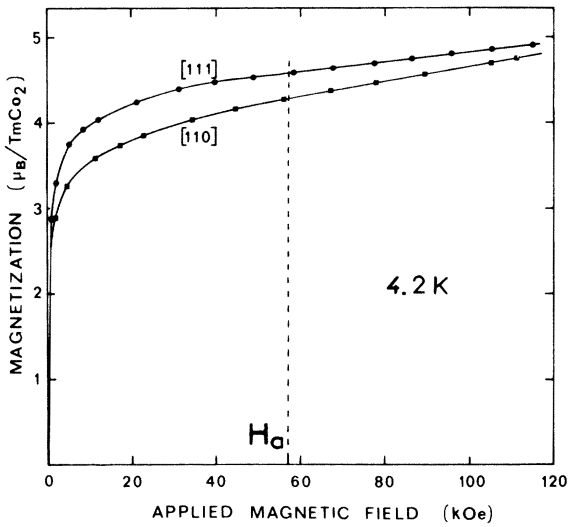

FIG. 1. Magnetization curves of the studied $TmCo_2$ single crystal along the [111] and [110] directions, at 4.2 K. H_a is the applied field in the neutron experiments.

$$R = \left(\frac{1+\gamma}{1-\gamma}\right)^2, \tag{1}$$

where $\gamma = F_M/F_N$, and F_M and F_N are the magnetic and nuclear structure factors, respectively. In the cubic $MgCu_2$-type structure, there are six different types of structure factors, depending on the values of h, k, and l, as shown in Table I.

TABLE I. Relations between h, k, l and the nuclear structure factors F_N for the $MgCu_2$-type Laves phases.

Conditions on h, k, l		F_N	Type
h, k, and l $= 2n$	h or k or $l \neq 4n$ and $h+k+l = 4n$	$\pm 8b_{Tm}$	I
	h, k, and $l = 4n+2$	$16b_{Co}$	II
	h, k, and $l = 4n$ and $h+k+l = 8n$	$8b_{Tm} + 16b_{Co}$	III
	h, k, and $l = 4n$ and $h+k+l = 8n+4$	$-8b_{Tm} + 16b_{Co}$	IV
h, k, and l $= 2n+1$	$\frac{5}{8}(h+k+l) = 8n \pm 1$ and $(h+k)$ or $(k+l) = 4n$ or $\frac{5}{8}(h+k+l) = 8n \pm 3$ and $(h+k)$ and $(k+l) = 4n+2$	$\pm 4\sqrt{2}\, b_{Tm} \pm 8b_{Co}$	V
	$\frac{5}{8}(h+k+l) = 8n \pm 1$ and $(h+k)$ and $(k+l) = 4n+2$ or $\frac{5}{8}(h+k+l) = 8n \pm 3$ and $(h+k)$ or $(k+l) = 4n$	$\pm 4\sqrt{2}\, b_{Tm} \mp 8b_{Co}$	VI

It is noteworthy that some structure factors are characteristic of Tm atoms only (type I) or of Co atoms only (type II). The magnetic structure factors corresponding to the localized magnetic densities are obtained from the nuclear structure factors by substituting $p_0\mu_{Tm}f_{Tm}(\vec{k})$ and $p_0\mu_{Co}f_{Co}(\vec{k})$ for the Fermi lengths b_{Tm} and b_{Co}, respectively; p_0 is the constant 0.2696×10^{-12} cm, μ_{Tm} and μ_{Co} are the magnetic moments per Tm and Co atoms expressed in Bohr magnetons, and $f_{Tm}(\vec{k})$ and $f_{Co}(\vec{k})$ are the Tm and Co form factors, for the scattering vector $\vec{k}$. In the subsequent tables and figures, we report the scattering amplitudes as the product μf for each atomic species.

Equation (1), which relates γ to the polarization ratio R, must be modified to take into account incomplete incident polarization and imperfect spin reversal. The corrections are smaller for values of R closer to 1. In the present experiment—using a CoFe polarizer—typical values of the polarizer, flipper, and analyzer efficiencies were, at 4.2 K, $P_0=0.993\pm0.002$, $P_f=0.993\pm0.001$, and $P_a=0.995\pm0.001$. At 100 K, the magnetic contributions are very weak and measurements were performed with a ^{57}Fe(Si) monochromator with which the intensity of the incident beam was multiplied by a factor of 4. In that case, P_0 was reduced to $P_0=0.962\pm0.002$. The half-wavelength contamination has also been taken into account. All these corrections have been evaluated as described in Ref. 12, and the resulting modifications of the γ values are always small. Other sources of possible error arise from perturbing characteristics of the sample, essentially depolarization and extinction. The depolarization of the incident beam has been measured on transmission through the sample. We have assumed a uniform-volume depolarization in order to make the necessary corrections. Typical values of this depolarization led to a reduction of the incident-beam polarization by a factor $P_d=0.996\pm0.002$. The extinction was determined from measurements at 4.2 K of the (111) and (022) reflections at five different wavelengths ranging from 0.7 to 1.2 Å. The extinction parameters[13,14] are the mosaic distribution $g=210\pm25$ and the size of blocks $t=1.1\pm4$ μm. Measurements at different wavelengths have shown that errors due to simultaneous reflections were negligible.

TABLE II. Corrected values of γ and values of the magnetic structure factors F_M for $TmCo_2$ at 4.2 K (type-II reflections excluded).

$h\ k\ l$	Type	$(\sin\theta)/\lambda$ (Å^{-1})	γ_{corr}	F_M (μ_B)
1 1 1	VI	0.121	5.28 ± 0.20	−36.8 ± 1.4
0 2 2	I	0.197	2.04 ± 0.05	−41.4 ± 1.0
3 1 1	V	0.231	1.27 ± 0.10	−27.7 ± 2.3
4 0 0	IV	0.279	7.55 ± 0.44	−41.6 ± 2.4
1 3 3	VI	0.304	3.90 ± 0.13	27.2 ± 0.9
4 2 2	I	0.342	1.55 ± 0.03	31.4 ± 0.6
5 1 1	V	0.363	0.74 ± 0.02	16.1 ± 0.6
3 3 3	V	0.363	0.68 ± 0.02	14.8 ± 0.6
0 4 4	III	0.395	0.561 ± 0.009	19.7 ± 0.3
5 3 3	V	0.458	0.624 ± 0.009	−13.6 ± 0.2
4 4 4	IV	0.483	4.57 ± 0.29	−25.2 ± 1.6
7 1 1	VI	0.498	2.33 ± 0.07	16.2 ± 0.5
1 5 5	VI	0.498	2.44 ± 0.09	−17.0 ± 0.6
3 5 5	V	0.536	0.491 ± 0.05	−10.7 ± 0.1
8 0 0	III	0.558	0.424 ± 0.009	14.9 ± 0.3
7 3 3	VI	0.571	1.95 ± 0.07	−13.6 ± 0.5
8 2 2	I	0.592	0.73 ± 0.03	−14.8 ± 0.6
0 6 6	I	0.592	0.66 ± 0.02	−13.4 ± 0.5
5 5 5	V	0.604	0.445 ± 0.009	9.7 ± 0.2
9 1 1	VI	0.636	1.64 ± 0.06	−11.4 ± 0.4
4 6 6	I	0.655	0.60 ± 0.01	12.2 ± 0.2
8 4 4	III	0.684	0.313 ± 0.006	11.0 ± 0.2
9 3 3	VI	0.694	1.48 ± 0.06	10.3 ± 0.4
1 7 7	VI	0.694	1.38 ± 0.07	9.6 ± 0.5
7 5 5	VI	0.694	1.46 ± 0.07	10.2 ± 0.5
3 7 7	V	0.722	0.308 ± 0.005	6.7 ± 0.1
1 1 1 1	V	0.774	0.262 ± 0.005	− 5.7 ± 0.1
5 7 7	V	0.774	0.285 ± 0.005	− 6.2 ± 0.1
0 8 8	III	0.789	0.225 ± 0.006	7.9 ± 0.2
9 5 5	VI	0.799	0.76 ± 0.04	− 5.4 ± 0.3
8 6 6	I	0.814	0.38 ± 0.01	− 7.7 ± 0.2
1 1 3 3	V	0.823	0.225 ± 0.005	4.9 ± 0.1
1 2 0 0	IV	0.837	1.83 ± 0.11	−10.1 ± 0.6
4 8 8	IV	0.837	1.47 ± 0.20	− 8.1 ± 1.1
7 7 7	VI	0.846	0.66 ± 0.03	− 4.6 ± 0.2
1 2 2 2	I	0.860	0.36 ± 0.01	7.4 ± 0.2
1 9 9	VI	0.891	0.56 ± 0.03	− 3.9 ± 0.2
1 3 1 1	V	0.912	0.207 ± 0.005	4.5 ± 0.1
1 1 5 5	V	0.912	0.174 ± 0.005	− 3.8 ± 0.1
3 9 9	V	0.912	0.184 ± 0.009	− 4.0 ± 0.2
1 2 4 4	IV	0.926	1.34 ± 0.20	− 7.4 ± 1.1
9 7 7	VI	0.934	0.53 ± 0.03	3.7 ± 0.2
1 3 3 3	V	0.954	0.184 ± 0.005	− 4.0 ± 0.1
5 9 9	V	0.954	0.170 ± 0.009	3.7 ± 0.2
8 8 8	III	0.967	0.139 ± 0.006	4.9 ± 0.2

III. RESULTS

In order to determine the Fermi lengths b and the Debye-Waller temperature factors B, a refinement of the crystallographic structure at room temperature was performed. The lattice parameter was found to be $a=7.166\pm0.001$ Å and with $b_{Co}=0.25\times10^{-12}$ cm,[15] the refinement led to the values $b_{Tm}=(0.686\pm0.002)\times10^{-12}$ cm for the crystal studied and $B_{Co}=0.54\pm0.01$, $B_{Tm}=0.64\pm0.01$, both in Å^2, at room temperature. The reliability factor is $R=0.7\%$.

TABLE III. Corrected values of γ and values of the magnetic structure factors F_M for $TmCo_2$ at 100 K (type-II reflections excluded).

hkl	Type	$(\sin\theta)/\lambda$ ($Å^{-1}$)	γ_{corr}	F_M (μ_B)
111	VI	0.121	0.578 ± 0.009	−4.03 ± 0.06
022	I	0.197	0.247 ± 0.001	−5.02 ± 0.03
311	V	0.231	0.145 ± 0.001	−3.16 ± 0.02
400	IV	0.279	0.85 ± 0.02	−4.67 ± 0.12
133	VI	0.304	0.461 ± 0.004	3.21 ± 0.03
422	I	0.342	0.194 ± 0.001	3.95 ± 0.03
511	V	0.363	0.121 ± 0.001	2.62 ± 0.02
333	V	0.363	0.115 ± 0.001	2.49 ± 0.02
044	III	0.395	0.094 ± 0.001	3.31 ± 0.04
533	V	0.458	0.101 ± 0.001	−2.19 ± 0.03
444	IV	0.483	0.54 ± 0.02	−2.97 ± 0.12
711	VI	0.498	0.287 ± 0.005	2.00 ± 0.03
155	VI	0.498	0.308 ± 0.006	−2.15 ± 0.04
355	V	0.536	0.077 ± 0.001	−1.67 ± 0.03
800	III	0.558	0.066 ± 0.001	2.32 ± 0.03
733	VI	0.571	0.223 ± 0.004	−1.56 ± 0.03
822	I	0.592	0.107 ± 0.001	−2.18 ± 0.02
066	I	0.592	0.106 ± 0.001	−2.16 ± 0.02
555	V	0.604	0.069 ± 0.001	1.49 ± 0.03
911	VI	0.636	0.225 ± 0.006	−1.57 ± 0.04
466	I	0.655	0.090 ± 0.001	1.83 ± 0.02
844	III	0.684	0.046 ± 0.003	1.62 ± 0.09
933	VI	0.694	0.190 ± 0.009	1.33 ± 0.06
177	VI	0.694	0.160 ± 0.013	1.16 ± 0.09
755	VI	0.694	0.156 ± 0.010	1.09 ± 0.07
377	V	0.722	0.045 ± 0.002	0.98 ± 0.04
1111	V	0.774	0.043 ± 0.003	−0.93 ± 0.06
577	V	0.774	0.040 ± 0.002	−0.88 ± 0.04
088	III	0.789	0.033 ± 0.002	1.15 ± 0.08
955	VI	0.799	0.109 ± 0.013	−0.76 ± 0.09
866	I	0.814	0.058 ± 0.005	−1.17 ± 0.10
1133	V	0.823	0.029 ± 0.004	0.63 ± 0.09
1222	I	0.860	0.049 ± 0.006	1.00 ± 0.12

Measurements of the polarization ratios of (hkk) reflections were made at 4.2 K out to $(\sin\theta)/\lambda = 0.967$ $Å^{-1}$ and at 100 K out to $(\sin\theta)/\lambda = 0.823$ $Å^{-1}$, in an applied magnetic field of 57.2 kOe. This highest value of the field was chosen in order to decrease the effects of the incident-beam depolarization by the sample. The corrected values of γ are listed in Tables II and III at 4.2 and 100 K, respectively, and in Table IV for the reflections of type II (no Tm contribution) at both temperatures. The values of the magnetic structure factors $F_m = \gamma F_N$, deduced from the data described above, are also presented in these tables. (The difference between B_{Tm} and B_{Co} has been neglected

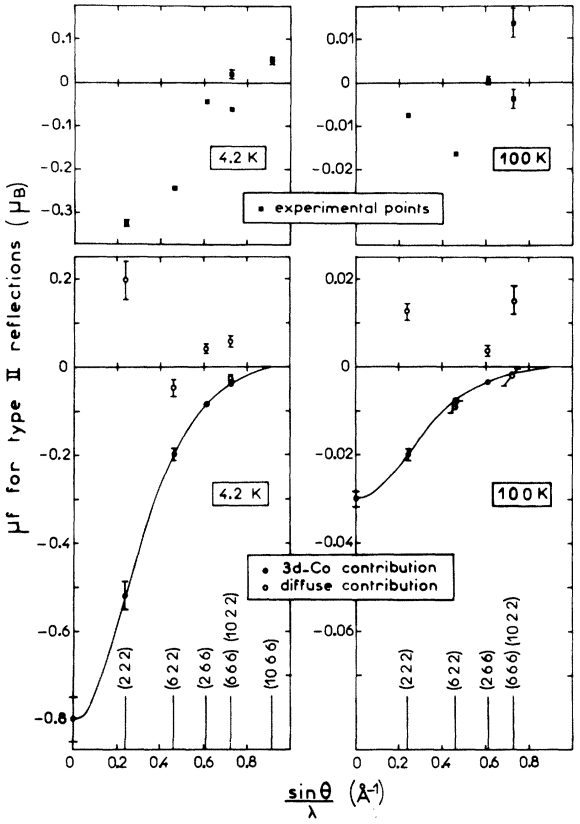

FIG. 2. Magnetic scattering amplitudes of type-II reflections at 4.2 and 100 K. Upper part: experimental points; lower part: decomposition of the experimental points into 3d-type and diffuse density contributions.

TABLE IV. Corrected values of γ and values of the magnetic structure factors F_M for type-II reflections of $TmCo_2$ at 4.2 and 100 K.

		$T = 4.2$K		$T = 100$K	
hkl	$(\sin\theta)/\lambda$ ($Å^{-1}$)	γ_{corr}	F_M (μ_B)	γ_{corr}	F_M (μ_B)
222	0.242	−0.351 ± 0.007	−5.20 ± 0.11	−0.0080 ± 0.0004	−0.118 ± 0.006
622	0.463	−0.265 ± 0.005	−3.92 ± 0.08	−0.0180 ± 0.0007	−0.266 ± 0.011
266	0.608	−0.049 ± 0.005	−0.72 ± 0.08	+0.0005 ± 0.0011	+0.008 ± 0.016
666	0.725	−0.067 ± 0.004	−0.99 ± 0.06	−0.004 ± 0.003	−0.06 ± 0.04
1022	0.725	+0.022 ± 0.011	+0.32 ± 0.16	+0.015 ± 0.003	+0.22 ± 0.05
1066	0.915	+0.055 ± 0.009	+0.82 ± 0.13	+0.015 ± 0.013	+0.22 ± 0.20

in this analysis.)

Figure 2 (top) shows the magnetic scattering amplitudes for 1 Co atom, $F_m/16$, for the reflections of type II. The variation of these scattering amplitudes with $(\sin\theta)/\lambda$ is quite different at the two temperatures. Furthermore, although only Co atoms contribute to the magnetic structure factors of these reflections, a Co form factor, characteristic of $3d$ electrons, similar to that determined on Co metal,[15] cannot fit the experimental points at either temperature. In order to clarify this result, measurements of the magnetic structure factors of type-II reflections have been made in the same applied magnetic field at various temperatures (15, 25, 50, 75, 125, and 250 K). Type-I reflections have also been studied to determine the Tm magnetic moment at each temperature. Results are collected in Table V. Between 25 and 125 K, the $(\sin\theta)/\lambda$ dependence of the magnetic scattering amplitudes of type-II reflections remains almost unchanged.

IV. ANALYSIS

A. Magnetic density at 4.2 K

The magnetic structure factors at 4.2 K have been used to make a projection of the moment density on the $(01\bar{1})$ plane which is reproduced in Fig. 3 (top). For convenience, a tetragonal cell has been chosen, the dimensions of which are a, $a/\sqrt{2}$, and $a/\sqrt{2}$. In order to avoid oscillations due to series-termination errors, we have used the classical average technique.[16] The average was taken over a volume of the same geometrical shape as the chosen cell, with sides of length 2δ times the cell parameters. The δ value corresponding to Fig. 3 is 0.03. For the (000) reflection, we have used the magnetic structure factor associated with a magnetization of $(4.3\pm0.1)\mu_B/TmCo_2$, given by the magnetic measurements.

The projected density along the line $Y=0.25$ is also plotted (Fig. 3, bottom). Tm atoms appear as well-localized regions of strong positive intensity. A negative magnetic density is also observed on the Co sites. The resulting value of all localized moments in one cell has not been evaluated by the local-moment calculation[16] because it cannot be assumed that the magnetic density between atomic sites is constant. Especially the magnetic scattering amplitudes measured on type-II reflections are not characteristic of a $3d$ moment. However, the Fourier projection gives evidence for a magnetic density on the Co sites very similar to that of a $3d$-type moment. We have evaluated the importance of this contribution by searching for the value of a $3d$-type moment that cancels it on the Fourier projection. At

TABLE V. Corrected values of γ and values of the magnetic scattering amplitudes μf for type-II and some type-I reflections of $TmCo_2$ at various temperatures.

T (K)		Type-II reflections (2 2 2)	(6 2 2)	(2 6 6)	(6 6 6)	(10 2 2)	Type-I reflections (0 2 2)	(0 6 6)
15	γ_{corr}	−0.166 ±0.001	−0.164 ±0.002	−0.017 ±0.002			1.59 ±0.03	0.60 ±0.02
	μf (μ_B)	−0.154 ±0.001	−0.152 ±0.002	−0.016 ±0.002			4.03 ±0.08	1.52 ±0.05
25	γ_{corr}	−0.073 ±0.003	−0.116 ±0.002	−0.003 ±0.002	−0.039 ±0.003	+0.040 ±0.002		0.472 ±0.008
	μf (μ_B)	−0.068 ±0.003	−0.107 ±0.002	−0.003 ±0.002	−0.036 ±0.003	+0.037 ±0.002		1.198 ±0.020
50	γ_{corr}	−0.033 ±0.001	−0.056 ±0.001	−0.001 ±0.002	−0.022 ±0.002	+0.022 ±0.002	0.57 ±0.01	0.243 ±0.005
	μf (μ_B)	−0.031 ±0.001	−0.052 ±0.001	−0.001 ±0.002	−0.020 ±0.002	+0.020 ±0.002	1.453 ±0.025	0.618 ±0.012
75	γ_{corr}	−0.017 ±0.002	−0.029 ±0.002	−0.001 ±0.002	−0.012 ±0.002	+0.013 ±0.002	0.357 ±0.006	
	μf (μ_B)	−0.016 ±0.002	−0.027 ±0.002	−0.001 ±0.002	−0.011 ±0.002	+0.012 ±0.002	0.907 ±0.015	
125	γ_{corr}	−0.0038 ±0.0010	−0.0102 ±0.0010	−0.0025 ±0.0030	−0.0032 ±0.0020	+0.0081 ±0.0020	0.197 ±0.003	
	μf (μ_B)	−0.0035 ±0.0010	−0.0094 ±0.0010	−0.0023 ±0.0030	−0.0030 ±0.0020	+0.0075 ±0.0020	0.500 ±0.008	
250	γ_{corr}	+0.0079 ±0.0010	0.0 ±0.001	0.0 ±0.003	+0.0013 ±0.0030	+0.0050 ±0.0030	0.093 ±0.002	
	μf (μ_B)	+0.0073 ±0.0010	0.0 ±0.001	0.0 ±0.003	+0.0012 ±0.0030	+0.0046 ±0.0030	0.236 ±0.004	

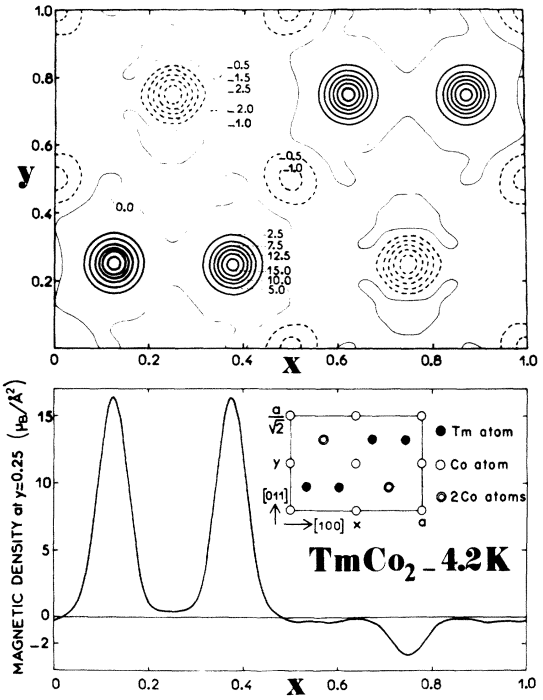

FIG. 3. Projection of the average density on the (01$\bar{1}$) plane at 4.2 K. Upper part: contour map. Numbers on contour lines are in units of $\mu_B/Å^2$. Thick lines are positive contours, thin lines zero contours, and dashed lines are negative contours. Lower part: projected density along the line $Y = 0.25$ as shown on the sketch of the corresponding atomic projection (insert).

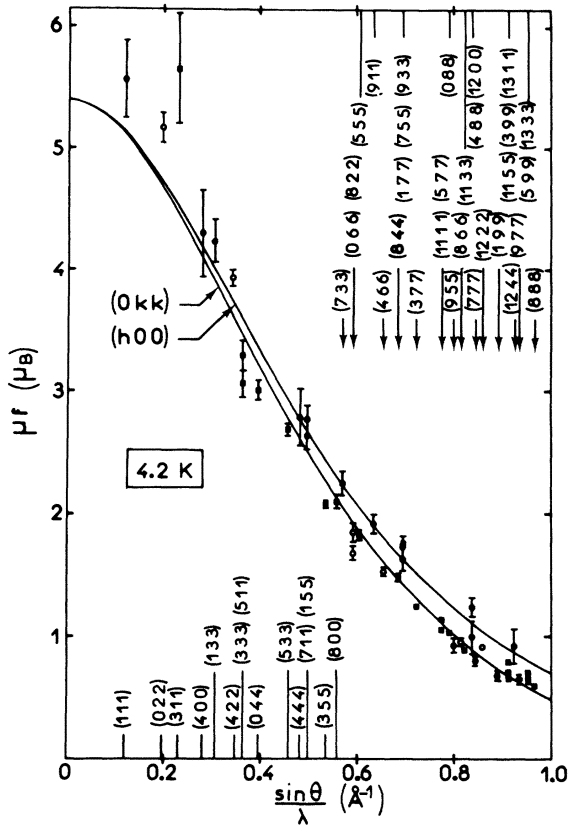

FIG. 4. Magnetic scattering amplitudes at 4.2 K for reflections with a Tm contribution. These amplitudes are obtained by subtracting the 3*d* Co magnetic contribution and are reduced to 1 Tm atom. Type-I reflections, open circles; type-IV and VI reflections, dark circles; type-III and -V reflections, dark squares. Full lines represent the Tm form-factor variations calculated at 4.2 K for the $(h00)$- and $(0kk)$-type reflections. The calculation is performed with the parameters defined in the text: $W = 2.0$ K, $x = 0.78$, $H_a + H_m$ [parallel to (01$\bar{1}$)] = 170 kOe.

this temperature (4.2 K), the magnetic moment thus obtained is $\mu_{Co} = (0.80 \pm 0.05)\mu_B$. The 3*d* contribution for the type-II reflections was then subtracted from the experimental values of the magnetic scattering amplitudes. The resulting values (Fig. 2, bottom) change sign with increasing $(\sin\theta)/\lambda$ and are of the same order of magnitude as the experimental ones. They can be attributed to an oscillatory diffuse magnetic density as in $TbNi_2$.[17]

A similar procedure has been used to determine the Tm magnetic moment. A first evaluation was performed by attributing the Tm-metal form factor[18] to the Tm atoms. The Tm moment thus deduced is $5.7\mu_B$. This value indicates an important reduction of the Tm moment by the crystal-field effects (free-ion value: $7\mu_B$). The initially chosen form factor is therefore not appropriate.

A calculation of the Tm form factor was then undertaken in the tensor-operator method[19,20] as described by Lander *et al.*[18] for TmSb. The form factor may be written

$$f(\vec{k}) = \langle j_0 \rangle + c_2\langle j_2 \rangle + c_4\langle j_4 \rangle. \tag{2}$$

The $\langle j_t \rangle$ radial integrals have been determined by Desclaux and Freeman[21] using relativistic calculations. The coefficients c_t are related to the wave function $|\psi_e\rangle$ of the Tm energy levels. The perturbing Hamiltonian acting on the ground multiplets is

$$\mathcal{H} = W\left(x\frac{O_4}{F_4} + (1 - |x|)\frac{O_6}{F_6}\right) - g\mu_B \vec{J}(\vec{H}_m + \vec{H}_a). \tag{3}$$

This Hamiltonian depends on three parameters: the crystal-field coefficients W and x in the Lea-Leask-Wolf notation,[22] and the molecular field H_m. H_a is the applied magnetic field. A self-consistent calculation has been carried out; the three parameters are obtained by fitting the magnetization measurements[23] using the value of the Tm moment deduced from the Fourier projection

($5.7\mu_B$ for the first step). The Tm form factor can then be calculated and the Tm moment is reevaluated on the Fourier projection. The set of values finally obtained is $W = 2.0$ K, $x = 0.78$, and $H_a + H_m = 170$ kOe. The corresponding ground state in the crystal-field potential only is a singlet. Under our experimental conditions, the calculated moment[23] is parallel to the field applied along $[01\bar{1}]$ and its value if $5.4 \pm 0.1\mu_B$. At 4.2 K, the most important contribution to the form factor comes from the ground state. The set of parameters is obtained with a poor precision because, aroung these values, the form factor, and the magnetization as well, do not depend very sensitively on them.

The smooth Tm form-factor variations obtained for the reflections $(h00)$ and $(0kk)$ are drawn on Fig. 4. The magnetic scattering amplitudes obtained by subtracting the $3d$ Co magnetic contribution $[-0.8\mu_B/(\text{Co atom})]$, and reduced to 1 Tm atom are also plotted on this figure. The deviations at low $(\sin\theta)/\lambda$ indicate a diffuse magnetic density which is positive on the Tm sites. At high scattering angles, the observed anisotropy of the form factor is not always in agreement with the calculated one, especially for some precisely measured reflections at the same Bragg angle: (11 1 1) and (5 7 7) or (11 5 5) and (3 9 9). These effects must be attributed to the oscillatory density and are of the same order of magnitude as those directly observed on type-II reflections. The mean value of the diffuse density $[(0.5 \pm 0.3)\mu_B/TmCo_2]$ is given by the difference between the magnetization value $[(4.3 \pm 0.1)\mu_B/TmCo_2]$ and the value of the localized magnetic moment deduced from the polarized-neutron measurements $[5.4(\pm 0.1) - 2 \times 0.8(\pm 0.05) = (3.8 \pm 0.2)\mu_B/TmCo_2]$.

B. Magnetic density at 100 K

A Fourier projection of the magnetic density has been performed in the same way as at low temperature. The magnetic structure factor of the (000) reflection corresponds to the measured magnetization of $(0.73 \pm 0.01)\mu_B$. The density along $Y = 0.25$ is shown in Fig. 5 [top (a)]. The strong positive peaks correspond to the $4f$ Tm contribution. The Tm moment at 100 K and the associated form factor have been determined by canceling these Tm peaks in the same self-consistent manner as at 4.2 K. The thermal population of the excited levels has been taken into account. The W and x crystal-field parameters are those evaluated at 4.2 K. The total field $H_a + H_m$ obtained is 60 kOe and the Tm moment is $(0.72 \pm 0.01)\mu_B$.

Besides these peaks, oscillations are observed; they are essentially due to the effects of the large Tm contribution on series-termination errors.

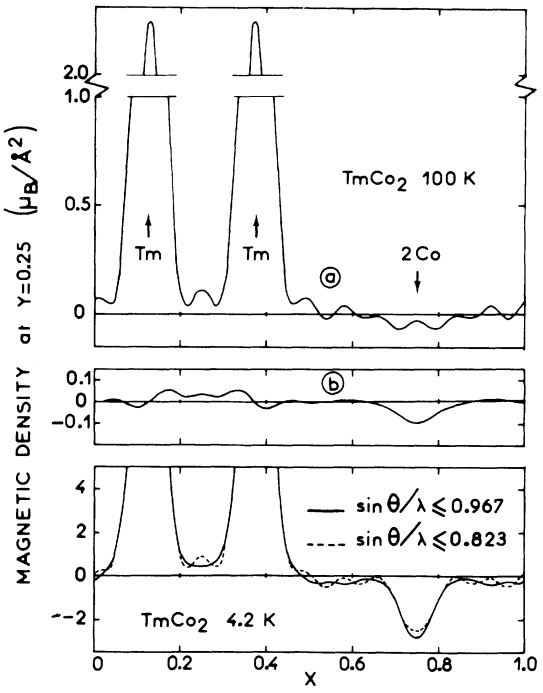

FIG. 5. Densities along the line $Y = 0.25$ (cf. Fig. 3) obtained by projections on the $(01\bar{1})$ plane. Upper part, 100 K: (a) directly observed density; (b) density found by canceling the Tm peaks. Lower part, 4.2 K: observed densities with reflections out to $(\sin\theta)/\lambda = 0.967$ (solid) and out to $(\sin\theta)/\lambda = 0.823$ (dashed).

This is illustrated (Fig. 5, bottom) by the comparison of the densities at 4.2 K obtained with reflections out to $(\sin\theta)/\lambda = 0.967$ Å^{-1} and out to $(\sin\theta)\lambda = 0.823$ Å^{-1} (same number of reflections as at 100K). Because of these strong oscillations, the direct analysis of the magnetic density on the Co sites is not possible. A Fourier difference projection has then been obtained by subtracting the Tm contribution. The density along $Y = 0.25$ [Fig. 5, top (b)] is now characterized by a weak moment localized on the Co sites with a value $(0.030 \pm 0.002)\mu_B$. As for 4.2 K, this $3d$ contribution has been subtracted from the experimental magnetic scattering amplitudes of type-II reflections (Fig. 2). The resulting magnetic scattering amplitudes show a $(\sin\theta)/\lambda$ dependence similar to that found at 4.2 K: They correspond to the same kind of diffuse magnetic density.

The comparison of the results at 4.2 and 100 K, presented in Fig. 2, shows that the $3d$ moment, relative to the diffuse magnetic density, is more important at 4.2 K than in the paramagnetic region. This explains the difference observed at low and high temperatures between the $(\sin\theta)/\lambda$ dependence of the magnetic scattering amplitudes of type-II reflections.

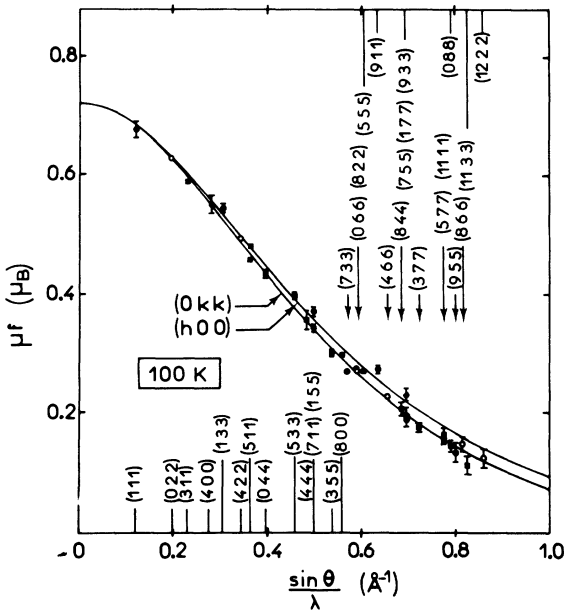

FIG. 6. Magnetic scattering amplitudes at 100 K for reflections with a Tm contribution. These amplitudes are obtained by subtracting the $3d$ Co magnetic contribution and are reduced to 1 Tm atom. Type-I reflections, open circles; Type-IV and VI reflections, dark circles; Type-III and V reflections, dark squares. Full lines represent the Tm form-factor variations calculated at 100 K for the $(h00)$- and $(0kk)$-type reflections. The calculation is performed with the parameters defined in the text: $W=2.0$ K, $x=0.78$, $H_a+H_m=60$ kOe.

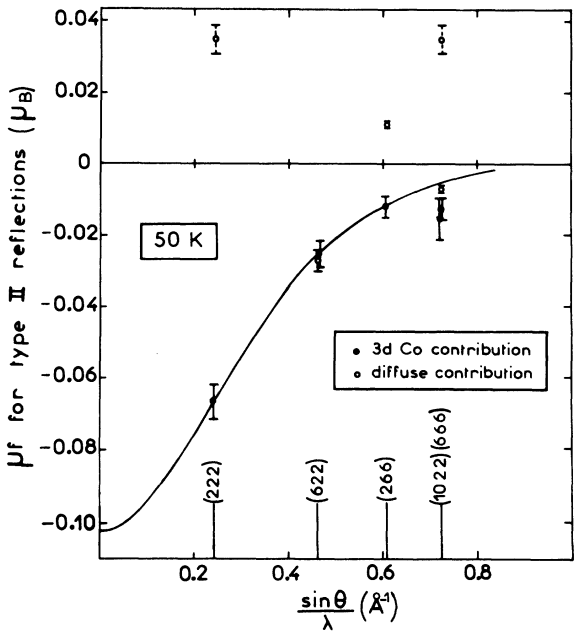

FIG. 7. Decomposition of the magnetic scattering amplitudes of type-II reflections at 50 K (see Table V) into two contributions: a diffuse density analogous to that determined at 100 K, and a $3d$-type Co moment.

The magnetic scattering amplitudes obtained by subtracting the $3d$ Co contribution $[-0.030\mu_B/$(Co atom)] and reduced to 1 Tm atom are plotted on Fig. 6, as well as the smooth calculated Tm form factors drawn for the $(h00)$ and $(0kk)$ reflections.

C. Cobalt paramagnetic susceptibility

At all temperatures, the magnetic density in $TmCo_2$ results from three contributions: a preponderant $4f$-type moment on the Tm sites, a $3d$-type moment on the Co sites, and a diffuse magnetic density which, as already noticed, is similar at 4.2 and 100 K. The $3d$ Co moment at the other temperatures (15 to 250 K) has been evaluated by considering the observed magnetic scattering amplitudes of type-II reflections as a sum of two components: the $3d$-type moment and a diffuse magnetic density analogous to that deduced at 100 K. This decomposition is illustrated on Fig. 7 at 50 K. The Co moments deduced at each temperature are plotted versus the corresponding Tm moment on Fig 8, and their values are listed in Table VI. Except for the points at 4.2 and 15 K, they almost lie on a straight line.

This result can be explained in the molecular-field model, in which the Co magnetic moment μ_{Co} may be written

$$\mu_{Co}=A[n_{CoTm}\mu_{Tm}+n_{CoCo}\mu_{Co}+H_a]\,, \tag{4}$$

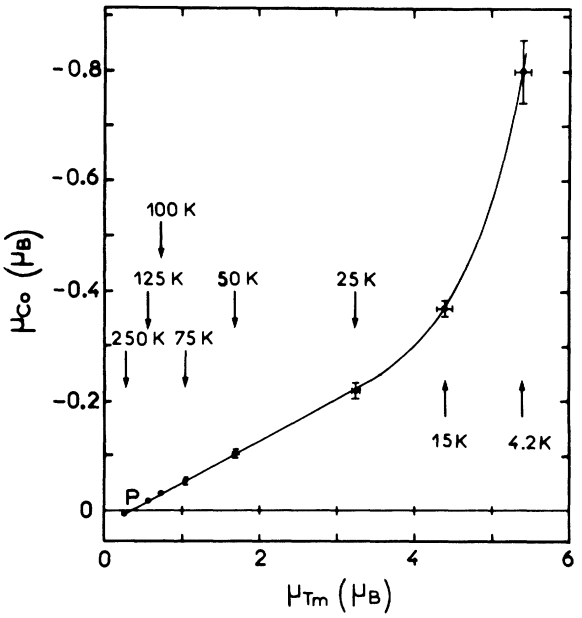

FIG. 8. Co magnetic moment versus the corresponding Tm moment measured at various temperatures.

TABLE VI. Co and Tm moments at various temperatures.

T (K)	μ_{Tm} (μ_B)	μ_{Co} (μ_B)
4.2	5.4 ±0.1	−0.80 ±0.05
15	4.4 ±0.1	−0.364 ±0.012
25	3.25 ±0.05	−0.214 ±0.013
50	1.68 ±0.03	−0.102 ±0.006
75	1.04 ±0.02	−0.053 ±0.006
100	0.72 ±0.01	−0.030 ±0.002
125	0.57 ±0.01	−0.016 ±0.003
250	0.270 ±0.005	+0.007 ±0.002

where n_{CoTm} and n_{CoCo} are the molecular-field coefficients between Tm and Co sublattices and inside the Co sublattice, respectively, μ_{Tm} is the Tm moment, H_a the applied field (57.2 kOe), and $A = C/T$ in the localized-electron model or $A = \chi_{Co}$ in the collective-electron model which implies the enhanced paramagnetism.[9] In both cases

$$\mu_{Co} = A'[n_{CoTm}\mu_{Tm} + H_a] \quad (5)$$

with

$$A' = \frac{A}{1 - An_{CoCo}} = \frac{C}{T - \theta}$$

in the first model (Curie-Weiss law) and $A' = \chi_y$ in the second model (χ_y weakly temperature dependent). Up to and including 125 K, the Co moment is coupled antiparallel to the Tm moment. On the contrary, at 250 K the Co moment is parallel to the applied field. The value of the Tm moment for which the Co moment is null [Fig. 8, point P: $\mu_{Tm} = (0.36 \pm 0.04)\mu_B$] leads to the determinination of n_{CoTm}, using relation (5): $n_{CoTm} = -H_a/\mu_{Tm} = -28 \pm 3$ emu/(Co atom). This coefficient is negative, in agreement with the ferrimagnetic structure at low temperature.

In the paramagnetic region, the variation of μ_{Co} with μ_{Tm} is linear. The thermal variation of the molecular-field coefficients being weak, A' is almost temperature independent. A Curie-Weiss law therefore cannot describe the thermal variation of the susceptibility of the Co sublattice. On the contrary, the enhanced-paramagnetism model is in agreement with such a variation ($A' \equiv \chi_y$). The value of this susceptibility is $\chi_y = (2.8 \pm 0.5) \times 10^{-3}$ emu/(Co atom). It is about twice as high as the YCo_2 susceptibility [1.6×10^{-3} emu/(Co atom) at 100 K].

Below 25 K (at 15 and 4.2 K) the increase of the Co moment with the Tm moment is much steeper (Fig. 8). At these low temperatures the Tm moment is more easily ordered under the effect of the applied field. Its more important magnetization creates a strong exchange field on the Co atoms. The resulting increase of the susceptibility is similar to the increase observed in YCo_2 in an applied field of 400 kOe.[24]

V. CONCLUSION

It has been possible by this polarized-neutron study of $TmCo_2$ to estimate the relative importance of three magnetic contributions: the rare-earth-localized $4f$ moment, the $3d$ collective-electron moment of the Co atom, and a diffuse magnetic density.

This diffuse density is oscillatory with distance. Magnetic interactions between Tm and Co atoms occur through the associated nonuniform polarization of the conduction electrons.

The large decrease of the Tm moment ($5.4\mu_B$) compared to the free-ion value is due to crystal-field effects; without any magnetic field the ground state is a singlet.

The Co susceptibility above 25 K is almost temperature independent. The Co behaves as a Pauli paramagnet under the action of two opposite fields: the molecular field due to Tm atoms and the applied field. Thus, we do not observed the characteristic temperature dependence expected from an intrinsic local moment on the Co atoms. The analysis of the paramagnetic susceptibility has then to be made on the collective-electron model. At 4.2 K a large increase of the Co susceptibility in the molecular field leads to a high value of the Co moment: $0.7\mu_B$. A possible relation between this property and the first-order ferri-paramagnetic transition observed in the compounds with Dy, Ho, and Er is being sought in studies now in progress of $HoCo_2$ and $TbCo_2$.

ACKNOWLEDGMENTS

Dr. R. Lemaire has proposed this subject and it is a pleasure to thank him for his suggestions and his constant interest in this study. We are very grateful to Dr. H. Levy for the precise determination of the crystallographic structure, Dr. P. J. Brown and Dr. J. X. Boucherle for providing us computing programs for the Fourier projections and for extinction corrections, to Dr. H. L. Davis for programs used in calculating the form factor, and to J. L. Sellers for technical assistance. Three of us (D.G., D.G., and F.G.) acknowledge with thanks the hospitality of the Solid State Division of the Oak Ridge National Laboratory during our tenure as guest scientists.

†Research sponsored by the U.S. Energy Research and Development Administration under contract with Union Carbide Corp.

[1]B. Barbara, D. Gignoux, D. Givord, F. Givord, and R. Lemaire, Int. J. Magn. 4, 77 (1973).
[2]R. Lemaire, Cobalt 33, 201 (1966).
[3]F. Givord and R. Lemaire, Solid State Commun. 9, 341 (1971).
[4]R. Lemaire and J. Schweizer, Phys. Lett. 21, 366 (1966).
[5]G. Petrich and R. L. Mössbauer, Phys. Lett. A 26, 403 (1968).
[6]F. Givord and J. S. Shah, C. R. Acad. Sci. B 274, 923 (1972).
[7]D. Bloch, D. M. Edwards, M. Shimizu, and J. Voiron, J. Phys. F 5, 1217 (1975).
[8]E. Burzo, Phys. Rev. B 6, 2882 (1972).
[9]D. Bloch and R. Lemaire, Phys. Rev. B 2, 2648 (1970).
[10]J. Deportes, D. Gignoux, and F. Givord, Phys. Status Solidi B 64, 29 (1974).
[11]J. Schweizer, thesis (University of Grenoble, Grenoble, France, 1968) (unpublished).
[12]R. M. Moon, W. C. Koehler, J. W. Cable, and H. R. Child, Phys. Rev. B 5, 997 (1972).
[13]W. H. Zachariasen, Acta Crystallogr. 23, 558 (1967).
[14]M. Bonnet, A. Delapalme, H. Fuess, and M. Thomas, Acta Crystallogr. B 31, 2233 (1975).
[15]R. M. Moon, Phys. Rev. 136, A195 (1964).
[16]R. M. Moon, Int. J. Magn. 1, 219 (1971).
[17]D. Givord, F. Givord, D. Gignoux, W. C. Koehler, and R. M. Moon, J. Phys. Chem. Solids (to be published).
[18]G. H. Lander, T. O. Brun, and O. Vogt, Phys. Rev. B 7, 1988 (1973).
[19]D. F. Johnston, Proc. Phys. Soc. Lond. 88, 37 (1966).
[20]S. W. Lovesey and D. E. Rimmer, Rep. Prog. Phys. 32, 333 (1969).
[21]J. P. Desclaux and A. J. Freeman (private communication).
[22]K. R. Lea, M. J. M. Leask, and W. P. Wolf, J. Phys. Chem. Solids 23, 1381 (1962).
[23]P. Bak, J. Phys. C 7, 4097 (1974).
[24]C. S. Shinkel (private communication).